

MESOPOROUS LiFeBO₃/C BY PECHINI SYNTHESIS FOR POSITIVE ELECTRODE IN LI-ION BATTERIES

V. J. GALLEGOS-SÁNCHEZ, L. C. TORRES-GONZÁLEZ, E. M. SÁNCHEZ, L. L. GARZA-TOVAR*

Universidad Autónoma de Nuevo León, Facultad de Ciencias Químicas, Av. Universidad S/N Cd. Universitaria, San Nicolás de los Garza, Nuevo León 66451, México

Synthesis of mesoporous LiFeBO₃/C composite has been achieved using Pechini sol-gel method. Thermal properties of fresh sol-gel samples were investigated by simultaneous thermogravimetric and differential thermal analysis (TGA-DTA). X-ray powder diffraction (XRD) and Fourier transform infrared spectroscopy (FT-IR) techniques were used for structural characterization of reaction products. Morphological and textural analysis of materials was carried out using Scanning electron microscopy (SEM) and Branauer Emmett Teller (BET) - Barrett-Joyner-Halenda (BJH) techniques. Temperatures between 550 and 650°C for 10h can help to produce almost pure LiFeBO₃/C with small amount of Fe₃BO₅ as impurity with surface area ~4.96 m² g⁻¹, and average pore size ~22.9 nm. Material tested in lithium cells delivers an initial discharge specific capacity of 213 mAhg⁻¹ and 170 mAhg⁻¹ in the 36th discharge at current density of 10 mA g⁻¹ with capacity retention of 80 %. The electrochemical performance of the electrode could be attributed to the surface area and mesoporosity as to the nano size particle.

(Received August 12, 2016; Accepted October 7, 2016)

Keywords: Pechini sol-gel; borates; LiFeBO₃/C; x-ray diffraction, textural properties

1. Introduction

Cathodes made of polyanionic compounds are attractive due to have more improved safety in comparison with cathodes made of transition metal oxides. Materials that contain polyanionic groups such as phosphates (PO₄), silicates (SiO₄), and borates (BO₃) have generated interest due to the inherent stability of polyanionic group versus the oxygen loss [1–4]. The presence of polyanionic groups such as (XO₄)^{y-} with strong X-O covalent bonds, increases the potential as a result of strong polarization of oxide ions through the X cation, decreasing the covalent character of the M-O bonds. Most lithium iron (II) phosphates works, reported the presence of FeO₆ octahedral as redox centers that show voltages within the range of 2.8 and 3.5 V versus Li/Li⁺ [1]. There is a need of alternatives for new better cathode materials that work at high operating voltages with high practical capacities. Borates could be a good alternative to phosphates, by having the lower weight BO₃³⁻ group related to PO₄³⁻, keeping the advantage of presenting higher working voltage and enhanced structural stability [5]. Among the new materials synthesized, only LiFeBO₃ possesses a high theoretical capacity of 220 mAhg⁻¹, and hence can be considered as a potential candidate for applications as cathode material in lithium ion batteries, besides that its chemical components are environment friendly, economical, and abundant in earth crust. Legagneur et al. have reported the performance of LiFeBO₃. They were able to de-intercalate only 0.04Li per formula [4]. This phase has been synthesized by solid state reaction [4–7] where Yamada et al.; achieved the highest specific capacity value of 190 mAhg⁻¹ at C/20 rate. They obtained such specific capacity of the composite of LiFeBO₃/C avoiding the exposition of material to moisture and air. The other method to obtain this phase utilized spray-drying [9], successfully obtaining the LiFeBO₃ phase with some impurity of α-LiFeO₂, which delivered an initial discharge

* Corresponding author: lorena.garzatv@uanl.edu.mx

capacity of $\sim 196.5 \text{ mAhg}^{-1}$ and presented a stable discharge performance of about $\sim 136.1 \text{ mAhg}^{-1}$ up to the 30th cycle at a discharge current density of 10 mA g^{-1} .

Nanostructured materials for lithium ion batteries have attracted much of interest in recent years due to its attractive properties such as specific surface area, short diffusion path for Li^+ compared with bulk materials. These characteristics can facilitate the charge transfer; enhance stability and specific capacity, even at high current rate during electrochemical reaction.

In this work, we present the results of the Pechini synthesis of a composite of LiFeBO_3/C . This technique allowed a homogeneous mixture of reagents, good stoichiometric control and low temperature of synthesis between 550 and 650 °C, producing small particles agglomerates with high porosity.

2. Experimental

2.1 Pechini Synthesis

The LiFeBO_3/C composite nanomaterials were obtained by Pechini method [9]. The starting reagents used during the synthesis were LiNO_3 (99 %, CTR Scientific), $\text{Fe}(\text{NO}_3)_3 \cdot 9\text{H}_2\text{O}$ (99.8 %, Fermont), H_3BO_3 (99.9 %, Fermont), Citric acid (CA) (99.9%, J. T. Baker) as the chelating agent and carbon source, ethylene glycol (EG) (99.4%, Fermont) as polymerization agent for polyesterification reaction. Fig. 1 shows the flow diagram corresponding to the LiFeBO_3/C synthesis by the Pechini method. About 150 mL of distillate water was used to dissolve iron (III) nitrate, lithium nitrate and boric acid under magnetic stirring for 30 min. In separated beakers, citric acid and ethylene glycol were dissolved in 100 mL of distilled water, and each reagent was dropped slowly into previous solution under stirring for 30 min. The temperature was then increased and kept between 80 and 90 °C until total evaporation of solvent and the formation of viscous resin. The obtained material product was dried at 100 °C for 3 h to eliminate remaining water, followed by a thermal treatment at 300 °C for other 3 h in a furnace for the decomposition of the organic components (citrates, ethylene glycol). Finally, the samples were ground using agate mortar; fine powders were pressed into pellets and calcined between 550 and 650 °C for 6-10 h using a tube furnace under flowing argon atmosphere.

2.2 Characterization

In order to determine heating temperatures for Pechini sol-gel samples, simultaneous thermal analysis TGA-DTA was carried out, using a SDT Q600 (TA-Instruments) analyser. The samples were analysed between room temperature ($\sim 25^\circ\text{C}$) up to 800 °C, using a heating rate of 5 °C/min under N_2 atmosphere. FT-IR measurements were performed on a Nicolet 380 FT-IR, Thermo Electron Corporation, in the 3500–400 cm^{-1} spectral range using attenuated total reflection ATR. Identification of crystalline phases of the synthesized materials was performed using powder X-ray diffraction (XRD), on a D2-Phaser diffractometer (Bruker) with $\text{Cu K}\alpha$ radiation with $\lambda = 1.5418\text{\AA}$, within 2θ range 10 to 90°. The specific surface area of nanomaterials was obtained with liquid nitrogen physisorption using textural analyser Nova 2000e by Quantachrome Instruments. To examine the morphology and size of the particles in synthesized powder, field emission-scanning electron microscopy (FE-SEM) with Nova Nano SEM 200 from FEI Company coupled with EDXS detector and transmission electron microscopy with CM-200 TEM from PHILIPS with 200kV maximum voltage, were used.

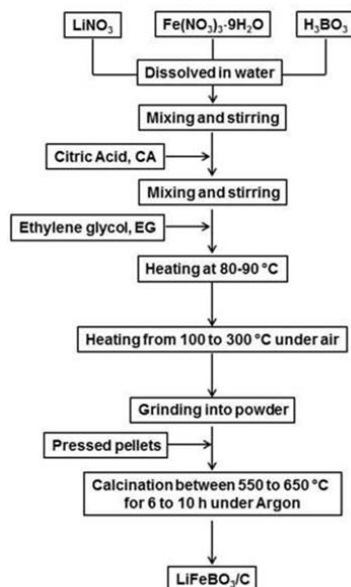


Fig. 1. Scheme for LiFeBO_3/C Pechini synthesis.

2.3 Electrochemical tests

Cathode materials were prepared by mixing appropriate amounts of active material (LiFeBO_3/C), acetylene black carbon and polyvinyl fluoride binder (PVDF), dispersed in *N,N*-dimethylacetamide using 80:5:15 weight %, respectively. The obtained slurry was coated over an aluminium foil by a doctor blade, producing a thin layer of about 10 μm thickness. Then materials were dried at 100°C under vacuum for 24 h. The electrodes were cut into disk shape (~12 mm), weighted and introduced into a glove box (Vac Atmospheres, OMNI-LAB) under argon atmosphere for battery assembling. Electrochemical measurements were carried out using a Biologic Mac Pile II Potentiostat. Coin cells CR2320 were built using the active material (LiFeBO_3/C) as cathode electrode, 1M LiPF_6 in (1:1:1) solution mixture of Ethylene Carbonate, (EC); Dimethyl Carbonate, (DMC); Diethyl Carbonate, (DEC); as electrolyte, polypropylene film as separator both from MTI Corporation and Li metal as anode, from Aldrich. Galvanostatic experiments were carried out, using continuous method using different current densities of 5, 10 and 20 mA g^{-1} and voltage window between 1.5 and 4.5 V vs Li/Li^+ .

3. Results and discussions

3.1 Thermal Analysis

The TGA-DTA curves for composition obtained by the Pechini method are depicted in Fig. 2. As can be seen, from TGA curve, there are at least two main weight losses, between room temperature and 250°C, which results in a gradual weight loss of about ~18%. The weight losses could be associated with adsorbed water and water produced during the synthetic process. A second weight loss of ~27%, between 250 and 450°C, corresponds to the decomposition of precursors such as citrates and ethylene glycol [10]. On the other hand, in the DTA curve, various endothermic events were detected between room temperature and 450 °C (100, 150, 280, 310 and 350 °C) those are related to main weight losses. Due to increase of temperature, a slightly exothermic event is observed between 550 and 600°C with apparent no weight loss that can be attributed to a crystallization process. Final endothermic event above 650°C could be associated with melting of the material. Thermogravimetric carbon contents of ~4.3% was determined for the reaction product.

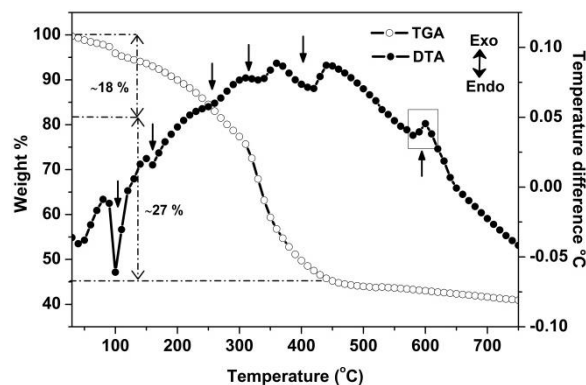


Fig. 2. TGA-DTA plots for 1:1 Fe:CA molar ratio fresh sample, under N_2 atmosphere.

3.2 FT-IR

Fig. 3 presents the FT-IR spectra of fresh and thermal treated samples. The transmittance spectra were recorded between the range of 3300 and 390 cm^{-1} . It can be observed that fresh sample Fig. 3(a) has a band about 3300 cm^{-1} and at 3200 cm^{-1} that can be associated with vibrational stretching mode of O–H group from water and ethylene glycol [11], bands nearby 1617 cm^{-1} and 1400 cm^{-1} could correspond to asymmetric and symmetric oscillations of carboxylic ions, respectively, confirming the chelation of metallic ions, [11, 12], within the range of 1200^{-1} – 1100 cm^{-1} . There is a band corresponding to C–O from groups COOH of citric acid. Characteristic bands from citric acid and ethylene glycol are shown between 812 and 650 cm^{-1} [13]. Bands below 650 cm^{-1} are assigned to metal-oxygen bond due to metallic ions and citric acid chelation [11, 12, 14]. Fig. 3b shows the spectrum obtained for sample heat treated at 300°C , observing a new band at 1900 cm^{-1} that can be related to C=O from the carboxylic acid group, no signal for O–H group belonging to water or ethylene glycol were observed and polymeric material signal was decreasing.

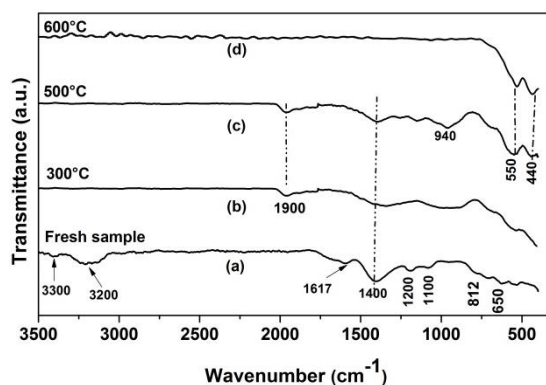


Fig. 3. FT-IR spectra for 1:1 Fe:CA molar ratio fresh and heat treated samples.

Fig. 3c shows the spectrum of the material heated up to 500°C , where a band at 940 cm^{-1} was detected, corresponding to the stretching mode of C–O bond, present in alcohols and the bands 550 and 440 cm^{-1} related to interactions metal-oxygen increasing as the temperature increases to 600°C (Fig. 3d), where only 550 cm^{-1} and 440 cm^{-1} bands were detected. Table 1 resumes FT-IR results obtained for different thermal treatment samples. These results indicate that only the materials calcined at 600°C are presented with metal-non-metal bonds that can be attributed to the formation of LiFeBO_3 compound. This also confirms that the information obtained by DTA-TGA indicating that near 600°C a crystalline phase is obtained.

Table 1. FT-IR spectral signals of 1:1 Fe:CA molar ratio composition at different thermal treatments.

Sample	Range cm^{-1}	Intensity	Assignment
Fresh	3300	w	O-H (water)
	3200	m	O-H (EG)
	1617	m	Asymmetric COO^-
	1400	s	(CA)
	1200	m	Symmetric COO^-
	1100	m	(CA)
	812-650	m	C-O (CA)
	<650	w	C-O (CA) (CA and EG)
300 °C	1900	m	Fe-O C=O (CA)
	1400	m	Symmetric COO^- (CA)
	1900	m	C=O (CA)
500 °C	1400	m	Symmetric COO^-
	940	m	(CA)
	550-440	m	C-O (EG)
	550-440	s	Fe-O
600 °C	550-440	s	Fe-O

w = weak, m = medium and s = strong

3.3 X-ray powder diffraction

The material was calcined at 550, 600 and 650 °C for 10 h, these temperatures were selected according to thermal analysis results. Fig. 4 presents the X-ray powder diffraction patterns obtained, it can be observed that material heat treated at 550°C for 10 h has reflections that agree with the reported LiFeBO_3 (ICDD 01-070-8321) [15]. As the temperature increases to 600 °C for 10 h, peaks seem to increase intensity, and this is related to an increase in crystallinity.

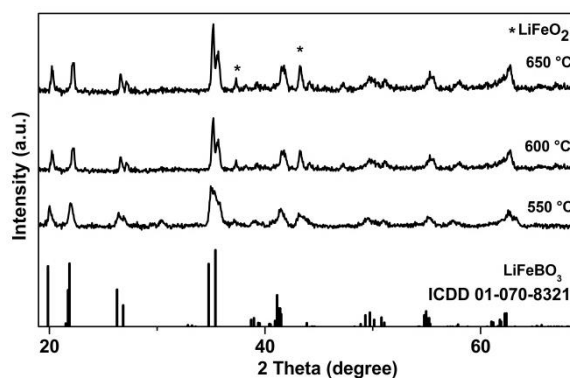


Fig. 4. X-ray powder diffraction patterns of LiFeBO_3/C composition, heat treated at 550, 600 and 650°C for 10h.

At 650 °C LiFeBO_3 crystalline phase is maintained with similar crystallinity, although a second crystalline phase Fe_3BO_5 , was also detected in minor concentration. It is suspected that the impurity could be formed due to the LiFeBO_3 phase instability in presence of oxygen and moisture. For this reason, samples were calcined and cooled under argon atmosphere and quickly analyzed and kept inside the glove box to prevent any undesirable reaction. The material heat treated at 600 °C for 10h, those patterns were identified as mixtures of the main phase LiFeBO_3 and an impurity of Fe_3BO_5 , (Vonsenite). Quantitative phase analysis using Topas software showed that impurity is present in less than 10%. Both materials agree well with 01-070-8321 and 00-025-0395 ICDD cards, with monoclinic (space group C2/c) and orthorhombic (space group Pbam) unit

cells, respectively. Results are comparable to previously reported by Yamada [5], they also achieved the LiFeBO_3/C composite with the presence of Fe_3BO_5 as secondary phase and one of the highest capacity 190 mAhg^{-1} .

3.4 Scanning electron microscopy

Fig. 5a-b shows two SEM micrographs of material synthesized at 600°C . It can be observed that materials have small particles, with different morphologies and sizes. Particles average sizes are between 187 and 362 nm. Some particle-forming clusters, showing porosity with porous size around 50 nm, which could be considered as mesoporous material.

Porosity can be attributed to CO_2 generation during the decomposition of metallic chelate Fe:CA , this porosity may improve the wetting properties and diffusion of electrolyte in the material being used as electrode in lithium ion battery.

This may lead to better contact between electrolyte and electrode allowing a high rate of discharge, and helping with minimizing volume distortion during cycling that is related to battery capacity fade. According to these properties, it could be expected a better performance material, allowing easy kinetics for lithium intercalation and improving stability among cycling with less distortion of material structure. Fig. 5c, corresponds to the STEM images of materials, show particle size between 73 and 142 nm with spherical shape and covered with carbon are observed for material. The carbon coating could be particularly effective to improve the electronic conductivity of the materials used as cathodes in lithium ion batteries [16, 17].

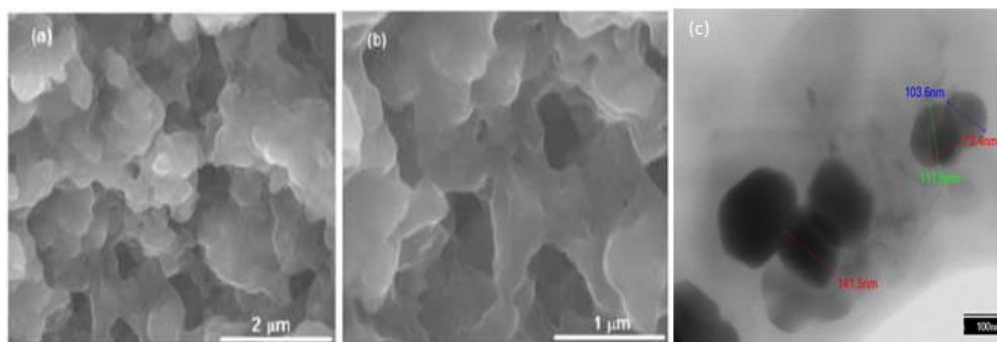


Fig. 5. SEM images of LiFeBO_3/C calcined at 600°C for 10h at a) $50,000\times$ b) $100,000\times$ and STEM imagen 5 (c) at $150,000\times$

3.5 BET-BJH

During the electrochemical reactions in the lithium ion batteries, lithium ions move from cathode to anode through the electrolyte, or vice versa. The ionic transfer from the cathode involves three steps: diffusion of lithium ions within the solid material (electrode), charge transfer reaction at the electrode-electrolyte interface and the motion of lithium ion through the electrolyte. Hence, surface area of active material and diffusion path of ions in the cathode are critical parameters for the performance of the lithium ion battery, especially knowing that diffusion of lithium ions is a determinant step in the kinetics of the lithium ion batteries.

Therefore, nanomaterials have been exhaustively investigated to improve the kinetic properties, i.e. decreasing diffusion length at nano scale [18-20]. Textural analysis of materials such as specific surface area and pore size distribution were carried out under Brunauer-Emmett-Teller (BET) and Barret-Joyner-Halenda (BJH) methods through adsorption-desorption of liquid nitrogen. Fig. 6 shows an adsorption-desorption nitrogen isotherm obtained for material. The isotherm corresponds to a IUPAC type IV with a H3 hysteresis type, indicating the existence of joined pores, one of the characteristics of mesoporous materials [21]. Pore size distribution was determined according to BJH method (insert figure 6), showing that around 75% of the pores are in the mesoporous region (within the range 2-50 nm), about 16% are in the macroporous range ($> 50 \text{ nm}$), and the rest ($< 2 \text{ nm}$) are in the microporous range.

The texture results show that materials have a mesoporous structure, that allows a better penetration of the electrolyte ions within the porous materials, improving the electrochemical performance of the electrodes [18, 22, 23]. On the other hand, specific surface area and average pore size determined with BET and BJH methods were $4.96 \text{ m}^2 \text{ g}^{-1}$, 22.9 nm, respectively. According to these results, we can conclude that Pechini method can be used to prepare materials with a surface area and porosity convenient for materials as cathodes in lithium ion batteries. Literature reports indicate that high surface area of active mesoporous materials allows a better impregnation and contact between electrolyte and cathode material, favor lithium ions access to cathode material, [18, 24] allowing superior electrochemical performance, i.e high specific capacity and capacity retention [24–26].

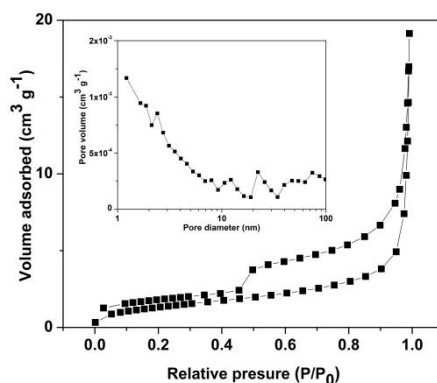


Fig. 6. N_2 adsorption/desorption curves of LiFeBO_3/C calcined at 600°C for 10h. Pore size distribution (insert).

3.6 Electrochemical tests

Electrochemical tests of LiFeBO_3/C compositions as cathode in lithium cell were carried out using a current density of 10 mA g^{-1} under charge/discharge cycles between 1.5 and 4.5 V. Fig. 7 shows the charge and discharge profiles for LiFeBO_3/C , using a current density of 10 mA g^{-1} , for 36 cycles, it can be observed that cell delivers a discharge capacity of about 213 mAh g^{-1} for the first cycle, corresponding to 97% of the theoretical capacity (220 mAh g^{-1}) which is better than previously reported [4-8] and discharge capacity of 193 mAh g^{-1} for the 20th cycle, meaning a capacity loss of 10%.

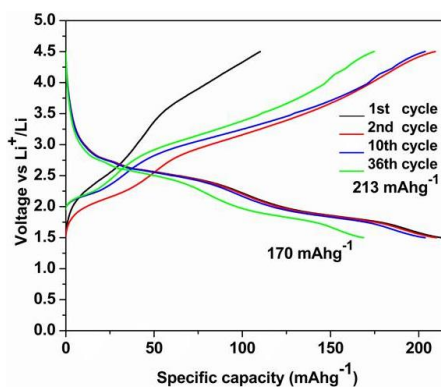


Fig. 7. Charge-discharge profiles of LiFeBO_3/C cell, cycled among 4.5-1.5V with density current of 10 mA g^{-1} .

A gradual loss of discharge capacity $\sim 170 \text{ mAh g}^{-1}$, was observed by the end of the 36th cycle. The improved behavior could be attributed to surface area and the mesoporosity allow an enhanced contact between interface electrode and lithium ions, showing a better electrochemical

performance: high discharge specific capacity and better capacity retention. The textural structure could enhance the electron transport, resulting in a higher discharge specific capacity. The Pechini technique was suitable for preparing mesoporous materials with nano size particles and carbon coatings promoting the charge transfer required for cathodes in lithium ion batteries.

4. Conclusions

Nanoporous composite of LiFeBO₃/C was successfully synthesized by applying the Pechini sol-gel technique using citric acid (CA) and ethylene glycol (EG). It was possible to determine different thermal events and propose reaction conditions from the TGA-DTA analysis of the product resin. From the structural results, phase formation was achieved using Fe:CA 1:1 molar ratios within the temperature range between 550 and 650°C for 10h. The composite displayed specific surface area and average pore size from 4.96 m² g⁻¹, 22.9 nm, respectively. The LiFeBO₃/C exhibited specific capacities of ~213 mAhg⁻¹ and 170 mAhg⁻¹ in the 36th discharge at current density of 10 mA g⁻¹ with capacity retention of 80 %. These results seem promising for the application of this material in lithium-ion batteries.

Acknowledgements

The authors would like to thank to SEP-CONACYT (CB-2012-01) for financial support through research project Ref. 189865, SEP-PROMEP, Ref. 103.5/12/7884 and the Universidad Autónoma de Nuevo León through PAICYT program. VJGS also thanks CONACYT for doctoral scholarship.

References

- [1] A. K. Padhi, K. S. Nanjundaswamy, J. B. Goodenough, *J. Electrochem. Soc.* **144**, 1188 (1997).
- [2] C. Masquelier, A. K. Padhi, K. S. Nanjundaswamy, J. B. Goodenough, *J. Solid State Chem.* **135**, 228 (1998).
- [3] A. Nyten, A. Abouimrane, M. Armand, T. Gustafsson, J. O. Thomas, *Electrochem. Commun.* **7**, 156 (2005).
- [4] V. Legagneur, Y. An, A. Mosbah, R. Portal, A. L. La Salle, A. Verbaere, D. Guyomard, Y. Piffard, *Solid State Ionics.* **139**, 37 (2001).
- [5] A. Yamada, N. Iwane, Y. Harada, S. Nishimura, Y. Koyama, I. Tanaka, *Adv. Mater.* **22**, 3583 (2010).
- [6] Y.Z. Dong, *J. of Alloys and Compd.* **461**, 585 (2008).
- [7] V. Aravindan, M. Umadevi, *Ionics.* **18**, 27 (2012).
- [8] B. Zhang, L. Ming, J. Zheng, J. Zhang, Ch. Shen, Y. Han, J. Wang, S. Qin, *J. Power Sources* **261**, 249 (2014).
- [9] J. Lin, M. Yu, C. Lin, X. Liu, *J. Phys. Chem. C* **111**, 5835 (2007).
- [10] L. da Conceição, N.F.P. Ribeiro, M. M.V.M. Souza, *Ceramics International.* **37**, 2229 (2011).
- [11] G. Socrates, 3rd edn. (John Wiley and Sons, 2001), p. 323.
- [12] G.V. Rama Rao, D.S. Surya Narayana, U.V. Varadaraju, G.V.N Rao, S. Venkadesan, *J. Alloys and Compd.* **217**, 200 (1995).
- [13] Y. Ochoa, Y.O., M. Vargas, J. E. Rodríguez Páez, *Revista Latinoamericana de Metalurgia y Materiales.* **3**, 931 (2009).
- [14] K. Nakamoto, 4th edn. (John Wiley and sons, 1986), p. 106.
- [15] JCPDS, Joint Committee on Powder Diffraction Standards, International Center For Diffraction Data, (2005)
- [16] J. Wang, J. Yang, Y. Tang, J. Liu, Y. Zhang, G. Liang, M. Gauthier, Y. K. Chen-Wiegart, M. Norouzi Banis, X. Li, R. Li, J. Wang, T. K. Sham, X. Sun, *Nature Communications.*

- 3415**, 1 (2014).
- [17] A. Abouimrane, M. Armand, and N. Ravet, *Proc. Electrochem. Soc.* **20**, 15 (2003).
- [18] P.G. Bruce, B. Scrosati, and J.-M. Tarascon, *Angew. Chem. Int. Ed.* **47**, 2930 (2008)
- [19] R. Mukherjeea, R. Krishnanb, L. Toh-Ming, N. Koratkar, *Nano Energy*. **1**, 518 (2012).
- [20] D. Kushnir, B.A. Sandén, *J. Clean Prod.* **19**, 1405 (2011).
- [21] K.S.W. Sing, D.H. Everett; R.A.W. Haul, L. Moscou, R. A. Pierotti, J. Rouquerol, T. Siemieniewska, *Pure Appl. Chem.* **57**, 603 (1985).
- [22] J. Cho, *J. Mater. Chem.* **20**, 4009 (2010).
- [23] C. Zhao, L. Liu, H. Zhao, A. Krall, Z. Wen, J. Chen, P. Hurley, J. Jiang, Y. Li, *Nanoscale*. **6**, 882 (2014).
- [24] Y. Fu, H. Jiang, Y. Hu, L. Zhang, C. Li, *J. Power Sources*. **261**, 306 (2014).
- [25] X. Zhu, X. Li, Y. Zhu, S. Jin, Y. Wang, Y. Qian, *J. Power Sources*. **261**, 93 (2014).
- [26] G. Qin, Q. Ma, C. Wang, *Electrochim. Acta.* **115**, 407 (2014).